L. Shalalfeh, P. Bodgan, and E. Jonckheere, ``Modeling of PMU data using ARFIMA models, *Clemson University Power System Conference,* Paper Session T-M II: Phasor Measurement Units (PMUs), Charleston, SC, September, 2018.

Modeling of PMU Data Using ARFIMA Models

Laith Shalalfeh
Dept. of Energy Engineering
German Jordanian University
Amman, Jordan
laith.shalalfeh@gju.edu.jo

Paul Bogdan*
Dept. of Electrical Engineering
University of Southern California
Los Angeles, California 90089
pbogdan@usc.edu

Edmond Jonckheere†
Dept. of Electrical Engineering
University of Southern California
Los Angeles, California 90089
jonckhee@usc.edu

***Abstract*—Installing Phasor Measurement Units (PMUs) in the smart grid has played an important role in having more reliable and secure grid. Due to the high sampling rate (50 samples/s), PMU generates massive amount of data compared to the conventional SCADA system. Understanding the mathematical and statistical characteristics of the PMU data is a very crucial step to perform accurate modeling and estimation of the power system variables (Voltage (V), frequency (f), and phase angle (θ)). In this paper, we show the non-stationarity of the PMU data by applying Augmented Dickey-Fuller and Kwiatkowski-Phillips-Schmidt-Shin tests on a large data set from the EPFL campus grid. Then, we study the fractality of the PMU data by estimating the differencing parameter (d) in the Autoregressive Fractionally Integrated Moving Average (ARFIMA) model. Our results call for adoption of ARFIMA models to model the PMU data in the smart grid.**

I. Introduction

Toward more reliable and secure power grid, the smart grid concept has been introduced to revolutionize and overcome several challenges and drawbacks in the conventional grid. The smart grid plays an important role in integrating the renewable energy resources and accommodating the increasing number of electric vehicles. Additionally, the installation of advanced control and wide-area monitoring systems as part of the smart grid development is essential for more reliable and resilient grid. Wide-area monitoring can be achieved via advanced sensing devices, such as Phasor Measurement Units (PMUs), installed at critical locations in the transmission system of the grid. Recently, new high precision PMUs, known as micro-PMUs (μPMUs) have been installed in the distribution system [1].

The first prototype of PMU was introduced by researchers at Virginia Tech in the early 1980s [2]. The PMU is a device that produces synchronized measurements of magnitude, phase angle, and frequency of voltage and current signals [3]. The synchronization is achieved using common time source provided by Global Positioning System (GPS). The PMUs have higher sampling rate of $30 - 50$ samples per second compared to the conventional Supervisory Control And Data Acquisition (SCADA) system. The high sampling rate enhances the visibility of the fast dynamic events in the power grid. Moreover, the synchronized PMU data with high precision provide more accurate real-time monitoring of the smart grid.

∗ P. Bogdan acknowledges the support by US National Science Foundation (NSF) under Grant CyberSEES 1331610 and CNS/CPS CAREER 1453860.
† E. Jonckheere acknowledges the support by NSF grant CCF-1423624.

The rapid increase in number of installed PMUs has produced massive amount of data measurements from all over the grid. These data have been exploited extensively to improve the power system operation and control by developing new algorithms and techniques in state estimation [4][5], event detection [6][7], model validation [8][9], and anomaly detection [10]. Furthermore, statistical analysis of PMU data has been used in stability and forecasting studies. The authors of [11] show the existence of self-organized criticality in blackout data. In [12], the authors show that the autocorrelation and variance of frequency increase as the system approach instability. The authors of [10] provide evidence of increasing Hurst exponent of the frequency as the Indian grid approaching the 2012 blackout.

In [13], we have shown that the PMU data (Voltage magnitude, frequency, and phase angle) possesses long-range memory using Detrended Fluctuation Analysis (DFA). ARFIMA modeling of the power loads was suggested in [14], consistently with the multi-fractality of such signals. Understanding the statistical characteristics of PMU data is of great importance due to several applications in power system studies.

In this paper, we study the fractality of PMU data by calculating the fractality parameters: scaling exponent (α), power exponent (β), and differencing parameter (d). Then, we show that Autoregressive Fractionally Integrated Moving Average (ARFIMA) model is the best model describing the short and long memories in PMU data based on the two information criteria: Akaike Information Criterion (AIC) and Bayesian Information Criterion (BIC).

The paper is organized as follows: In Sec.II, we study the stationarity of PMU data. Sec.III shows the fractality of PMU data by calculating the differencing parameter of PMU data. We determine the best ARFIMA model to fit the PMU data in Sec. IV. Sec.V is the conclusion.

II. Statistical Characteristics of PMU Data

We first provide a description of the PMU data and the power grid from which that data was collected. Then, we investigate the stationarity of the data using unit root tests.

A. Overview of PMU Data

Typical phasor measurement units provide measurements for the following variables in the power system: voltage (V), current (I), frequency (f), active power (P), and reactive

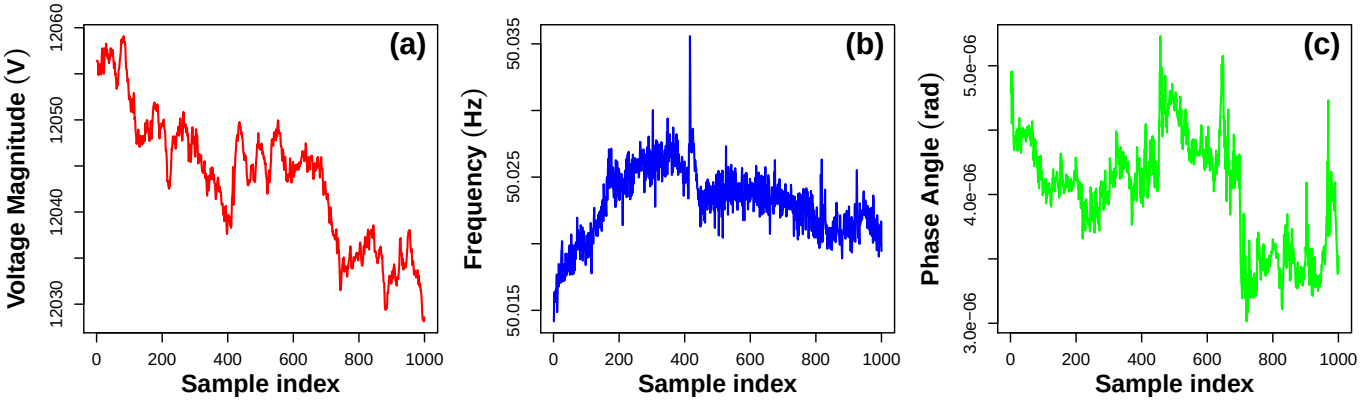

Fig. 1. PMU data collected from the EPFL campus grid in 2014: (a) Voltage magnitude time series (b) Frequency time series (c) Phase angle time series

power (Q). The measured voltages and currents are represented using the phasor format which consist of magnitude and phase angle. In this paper, we use data collected from EPFL campus grid as part of their real-time state estimation project [15]. The rated voltage magnitude (line-line) and frequency of the EPFL campus grid are 20 kV and 50 Hz, respectively. Several PMUs were installed throughout the campus grid to collect the data at sampling rate of 50 samples/s. We focus our analysis on a large data set of voltage magnitude (V), frequency (f), and phase angle (θ). The data set consists of 120,000 time series (1000 samples each) of the three variables collected from the campus grid in January, April, June, and December 2014 [16]. In Fig. 1, we show three 1000-sample time series of voltage magnitude (red), frequency (blue), and phase angle (green).

B. Stationarity

We study the stationarity of the PMU data using unit root tests. They can classify the time series as stationary or not based on the existence of unit root in the time series. Augmented Dickey-Fuller (ADF) and Kwiatkowski-Phillips-Schmidt-Shin (KPSS) are two of the most popular unit root tests, so we use them to check the stationarity of PMU data (V, f, θ).

1) Augmented Dickey-Fuller (ADF) Test: The ADF test can classify the time series as stationary or not using hypothesis testing. The null hypothesis (H_0) is that the time series is non-stationary and unit root exists. The alternative hypothesis (H_1) is that the time series is stationary.

We conduct the ADF test on 120,000 time series of PMU data ($V, f, and\ \theta$), each time series contains 1000 samples (20 seconds). Using the command "adf.test" in R software, we calculated the $p-$value for each time series to determine its stationarity. The percentages of time series with $p-$values above 0.01 (accept the null hypothesis (H_0)) and time series with $p-$values below or equal to 0.01 (reject the null hypothesis (H_0)) are shown in Table I.

The first column ($p-$value$>$ 0.01) under the ADF test in Table I shows that we can not reject the null hypothesis for most of time series. Not rejecting the null hypothesis in the ADF test indicates existence of unit root and non-stationarity of time series. Most of the voltage and frequency time series shows non-stationarity with percentages 88.16% and 96.86%, respectively. However, the phase angle time series show non-stationarity approximately for half the total number of time series.

2) Kwiatkowski-Phillips-Schmidt-Shin (KPSS) Test: It is another statistical test to study the stationarity of time series based on the unit root test. It is different than the ADF test in the sense that the null hypothesis (H_0) is the absence of the unit root and the alternative hypothesis (H_1) is the presence of unit root.

Similarly, we applied the KPSS test to 120,000 time series of PMU data. We used the command "KPSS.test" in R software to determine the stationarity by calculating the $p-$values. The percentages of time series with $p-$values above 0.01 (accept the null hypothesis (H_0)) and time series with $p-$values below or equal to 0.01 (reject the null hypothesis (H_0)) are shown in Table I.

The second column ($p-$value$\leq$ 0.01) under the KPSS test shows that most of PMU data are non-stationary. The percentage of non-stationary phase angle time series is the smallest (78.63%) and the percentage of non-stationary frequency is the highest (99.70%).The KPSS test provides a solid evidence for existence of unit root and non-stationarity of PMU data (V, f, and θ).

TABLE I. Percentages of stationary (2^{nd} and 3^{rd} columns) and non-stationary (1^{st} and 4^{th} columns) time series.

	ADF		*KPSS*	
	$p > 0.01$	$p \leq 0.01$	$p > 0.01$	$p \leq 0.01$
Voltage	88.16%	11.84%	05.48%	94.52%
Frequency	96.86%	03.14%	00.30%	99.70%
Angle	45.88%	54.12%	21.37%	78.63%

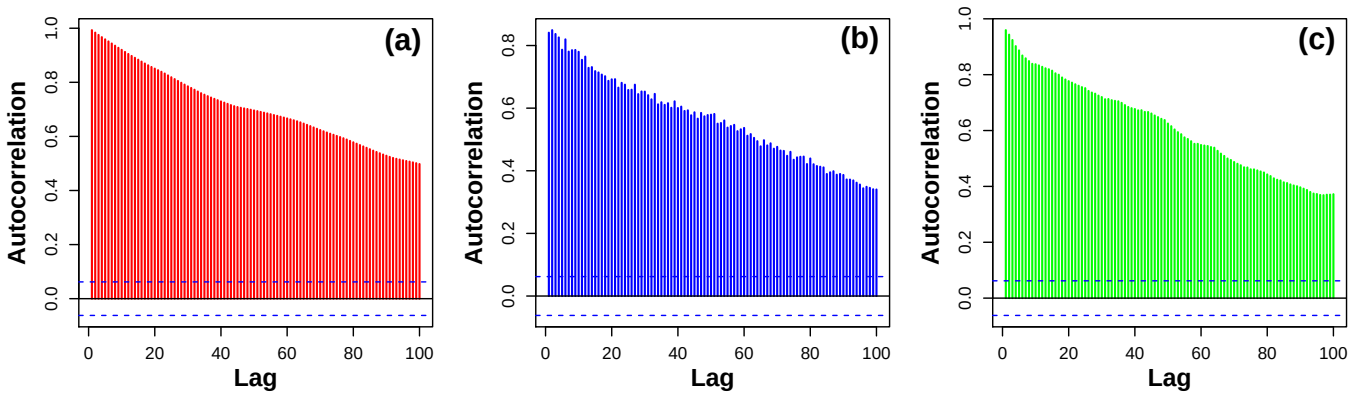

Fig. 2. Autocorrelation functions of PMU data: (a) Voltage magnitude (b) Frequency (c) Phase angle

III. Fractality of PMU Data

Fractal time series have the unique characteristics of exhibiting a slow (non-exponential) decay of the autocorrelation function (ACF), heavy-tailed probability density function (PDF), and power density function in the form $1/f^{\beta}$. The slow decay of the autocorrelation function indicates a long-range memory (dependence) in the time series represented by persistent correlation between the time series samples as the lag increases. Fractality has been observed in wind speed, brain signals, stocks market.

We investigate the fractality of PMU data by calculating their autocorrelation functions (ACFs). The autocorrelation functions of the voltage magnitude (red), frequency (blue), and phase angle (green) are shown in Figs. 2 (a)-(c), respectively. The autocorrelation functions show a slow hyperbolic decay compared to exponentially decaying random time series. The slow decay of the autocorrelation function could be a sign of the existence of long-range memory in the PMU data.

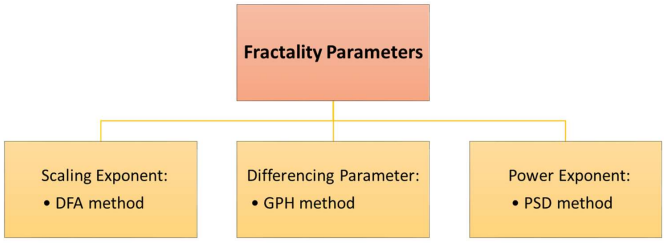

Fig. 3. Fractality Parameters

We quantify the fractality and long-range dependence in PMU data using fractality parameters, as shown in Fig. 3. These parameters are: Scaling exponent (α), Differencing parameter (d), and Power exponent (β). The relationships among these parameters for non-stationary time series are shown in Eq. (1):

$$d = \alpha - 0.5 = \beta/2. \tag{1}$$

In the bulk of this section, we estimate the three parameters of the PMU data using three methods: (1) Detrended Fluctuation Analysis (DFA), (2) Geweke and Porter-Hudak (GPH) method, and (3) Power Spectral Density (PSD) method.

A. Detrended Fluctuation Analysis (DFA)

DFA is a robust method to estimate the scaling exponent (α) for non-stationary time series. The method has been first introduced to study the long-range dependence of DNA nucleotides in 1994 [17]. One of the main advantages of DFA method is dealing with the non-stationarity in the data using detrending. The DFA has been used extensively to estimate the scaling exponent in several research areas. Based on the value of the scaling exponent, we can determine the statistical characteristics (stationarity and correlation) of the time series.

We applied the DFA method on the PMU data (V, f, and θ) to calculate the scaling exponent as shown in Table II. The results show that the voltage magnitude, frequency, and phase angle time series have average scaling exponents 1.18, 1.58, and 1.00, respectively. The results show that most of the time series are non-stationary ($\alpha \geq 1$) with scaling exponents between 1 and 1.58. Moreover, the data have long-range dependence ($\alpha \neq 0.5$) that is not following the power law. To model the PMU data, it would be important to estimate the differencing parameter (d) using Eq. (1). The distributions of the differencing parameter using DFA are shown in the first columns in Figs. 4 (a)-(c).

TABLE II. The means and standard deviations (in parentheses) of the scaling exponents (α) of voltage, frequency, and phase angle.

	Voltage	*Frequency*	*Angle*
Scaling exponent (α)	1.18 (0.18)	1.58 (0.21)	1.00 (0.27)

B. Geweke and Porter-Hudak (GPH) Method

GPH is a method to estimate the differencing parameter (d) of time series independently of DFA. It estimates the differencing parameter using linear regression of the log periodogram. The linear regression is performed in the low frequencies, so

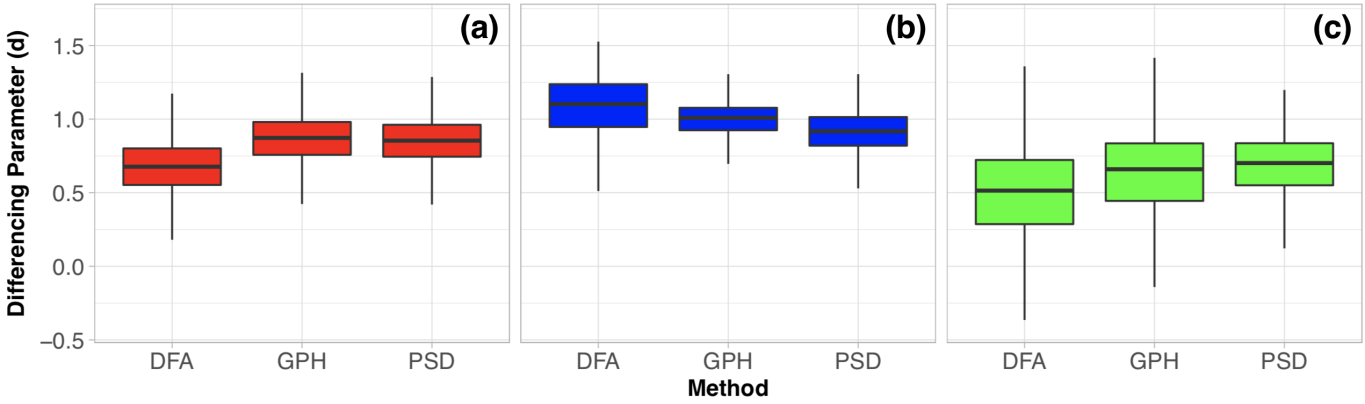

Fig. 4. Boxplots of differencing parameters of PMU data using DFA, GPH, and PSD: (a) Voltage Magnitude (b) Frequency (c) Phase Angle

these methods are suitable to estimate the differencing parameter in non-stationary time series. We calculate the differencing parameter of PMU data using the command 'fdGPH' from the package 'fracdiff' in R software. The results are shown in Table III. The differencing parameters of the PMU data have means between 0.5 and 1.0. Similarly, that indicates the non-stationarity ($d > 0.5$) and long-range memory ($d > 0$) of the PMU data. The distributions of the differencing parameters using GPH method are shown in the second columns in Figs. 4 (a)-(c) .

TABLE III. The means and standard deviations (in parentheses) of the differencing parameters (d) of voltage, frequency, and phase angle.

	Voltage	*Frequency*	*Angle*
Diff. parameter (d)	0.86 (0.17)	1.00 (0.14)	0.63 (0.26)

C. Power Spectral Density (PSD) Method

The PSD method [18] estimates the power exponent of non-stationary time series after some modifications to improve the accuracy of the PSD estimation. These modifications include detrending the data using bridge detrending and estimating the power exponent after excluding the high frequency component of the PSD. Using the R code in [19], we estimate the power exponent of PMU data as shown in Table IV. The power exponents have mean values between pink noise ($\beta = 1.00$) and brown noise ($\beta = 2$). It is clear from the power exponent values that the signals are not random ($\beta = 0$) and possesses a long-range memory. We further calculated the differencing parameters of the PMU data from the PSD method using Eq. (1). The distributions of the differencing parameter using the PSD are shown in the third column in Fig. 4 (a)-(c).

IV. ARFIMA Models of PMU Data

ARFIMA is a stochastic model introduced by Granger and Joyeux in 1980 [20]. This model is a generalization of the ARIMA model (d is integer) developed by Box and Jenkins [21] in the sense that the differencing parameter (d) could have a fractional (non-integer) values. The fractional ARIMA (ARFIMA) models were able to embody the long-range memory in the data by applying the fractional differencing. In case of nonlinearity, it appears that ARFIMA modeling can be enhanced with machine learning; however, here the degree of nonlinearity does not seem to require that machine learning enhancement. We adopt the ARFIMA models to capture the long-range memory in the PMU data (V,f, and θ).

TABLE IV. The means and standard deviations (in parentheses) of the power exponents (β) of voltage, frequency, and phase angle.

	Voltage	*Frequency*	*Angle*
Power exponent (β)	1.70 (0.33)	1.83 (0.29)	1.36 (0.40)

A. ARFIMA Model

Since most of the PMU data is non-stationary, we need to differentiate the PMU data to remove the non-stationarity as in the ARIMA models. In Sec. III, we have shown the existence of long-range memory in the PMU data by calculating the three fractality parameters (α, d, and β). Moreover, we can calculate the differencing parameter (d) from the scaling exponent (α) and power exponent (β) using Eq. (1).

Let X_t be a zero-mean time series with long-range memory. The ARFIMA(p, d, q) model of X_t is defined in Eq. (2):

$$\left(1 - \sum_{i=1}^{p} \Phi_i B^i\right)(1 - B)^d X_t = \left(1 + \sum_{i=1}^{q} \Theta_i B^i\right)\epsilon_t \quad (2)$$

B is the delay operator, d is the differencing parameter, and the term $(1 - B)^d$ is the difference operator ∇^d. The Φ_is are the Auto Regressive (AR) parameters and the Θ_is are the Moving Average (MA) parameters. $(1 - \sum_{i=1}^{p} \Phi_i B^i)$ is the autoregressive polynomial of order p and $(1 + \sum_{i=1}^{q} \Theta_i B^i)$ is

the moving average polynomial of order q. The uncorrelated, zero-mean residual is represented by ϵ_t.

The ARFIMA model becomes ARMA model when $d = 0$ and ARIMA models when d is integer. A time series with long-range memory has differencing parameter (d) between 0 and 0.5 if it is stationary and differencing parameter between 0.5 and 1 if it is non-stationary. The ARMA and ARIMA models can capture the short-range dependence only; however, the ARFIMA models with fractional d can capture both the short-range and long-range dependence. As expanded upon in this paper, the difficulty is to compute the d parameter. Once the latter is computed, the ARFIMA reduces to the classical Box-Jenkins ARMA modeling of $(1 - B)^d X_t$.

B. Model Estimation

The estimation of the ARFIMA model parameters is summarized in three steps. The first step is estimating the differencing parameter (d). Then, we fit the time series to ARFIMA(p, d, q) models using several combinations of autoregressive and moving average polynomials with different orders. We cover all the combinations of p and q between 0 and 2, like $(0, d, 0), (1, d, 0), (0, d, 1), ...(2, d, 2)$. Finally, we use the two information criteria (AIC and BIC) to compare the different models and choose the best fit.

We exploit the three steps mentioned above to find the best ARFIMA models that fit the PMU data. We have chosen three 1000-sample time series of voltage, frequency, and phase angle collected from the EPFL campus grid in 2014. We perform steps 1 and 2 using the command '$arfima$' from the 'arfima' package in R software. To calculate the values of the AIC and BIC information criteria in step 3, we use the commands 'AIC' and 'BIC' from the package 'stats' in R software.

A comparison between the different ARFIMA models of the voltage time series is shown in Table V. The results show that the best ARIFMA model to fit the voltage time series based on AIC and BIC values is ARFIMA$(0, d, 1)$. The model $(0, d, 1)$ has the lowest AIC and BIC values between the other models with values of -946.9 and -927.3, respectively. The parameters of the best fit of the voltage time series are $\Theta_1 = -0.63$ and $d = 0.89$.

In Table VI, we find the ARFIMA models of the frequency time series and their AIC and BIC values. The best fit of the frequnecy time series is ARFIMA$(1, d, 2)$ with AIC and BIC values of -13645.5 and -13616, respectively. The parameters of the model $(1, d, 2)$ are $\Phi_1 = -0.92$, $\Theta_1 = -0.18$, $\Theta_2 = 0.61$, and $d = 0.94$.

The ARFIMA models of the phase angle time series are shown in Table VII. The ARFIMA model $(1, d, 1)$ is the best fit of phase angle time series based on AIC value of -29543 and BIC value of -29518.5. The parameters of the best model to fit the phase angle time series are $\Phi_1 = -0.18$, $\Theta_1 = 0.18$, and $d = 0.83$.

V. Conclusion

The starting point of this paper has been evidence of non-stationarity in PMU data using unit root tests. We then followed up with the DFA that capitalizes on non-stationarity to compute the fractality parameters (α), showing existence of long-range memory in the PMU data. This is further confirmed by calculating the other fractality parameters (differencing parameter d, and power exponent β), showing consistency among different methods. Since most of the PMU data is non-stationary, we need to differentiate the PMU data to remove the non-stationarity, resulting in the ARFIMA model of the PMU data. The next challenge is to formulate some *"first principles"* that could justify such model.

References

[1] A. von Meier, D. Culler, A. McEachern, and R. Arghandeh. Micro-synchrophasors for distribution systems. In *ISGT 2014*, pages 1–5, Feb 2014.

[2] A. G. Phadke and J. S. Thorp. *Synchronized phasor measurements and their applications*. Springer Science & Business Media, 2008.

[3] IEEE standard for synchrophasor data transfer for power systems. *IEEE Std C37.118.2-2011 (Revision of IEEE Std C37.118-2005)*, pages 1–53, Dec 2011.

[4] W. Jiang, V. Vittal, and G. T. Heydt. Diakoptic state estimation using phasor measurement units. *IEEE Transactions on Power Systems*, 23(4):1580–1589, Nov 2008.

[5] Liang Zhao and A. Abur. Multi area state estimation using synchronized phasor measurements. *IEEE Transactions on Power Systems*, 20(2):611–617, May 2005.

[6] J. E. Tate and T. J. Overbye. Line outage detection using phasor angle measurements. *IEEE Transactions on Power Systems*, 23(4):1644–1652, Nov 2008.

[7] L. Xie, Y. Chen, and P. R. Kumar. Dimensionality reduction of synchrophasor data for early event detection: Linearized analysis. *IEEE Transactions on Power Systems*, 29(6):2784–2794, Nov 2014.

[8] Y. Zhang, E. Muljadi, D. Kosterev, and M. Singh. Wind power plant model validation using synchrophasor measurements at the point of interconnection. *IEEE Transactions on Sustainable Energy*, 6(3):984–992, July 2015.

[9] J. Chen, P. Shrestha, S. H. Huang, N. D. R. Sarma, J. Adams, D. Obadina, and J. Ballance. Use of synchronized phasor measurements for dynamic stability monitoring and model validation in ercot. In *2012 IEEE Power and Energy Society General Meeting*, pages 1–7, July 2012.

[10] L. Shalalfeh, P. Bogdan, and E. Jonckheere. Kendall's tau of frequency hurst exponent as blackout proximity margin. In *2016 IEEE International Conference on Smart Grid Communications (SmartGridComm)*, pages 466–471, Nov 2016.

[11] B. Carreras, D. Newman, I. Dobson, and A. B. Poole. Evidence for self-organized criticality in a time series of electric power system blackouts. *IEEE Transactions on Circuits and Systems*, 51(9), September 2004.

[12] E. Cotilla-Sanchez, P. D. H. Hines, and C. M. Danforth. Predicting critical transitions from time series synchrophasor data. *IEEE Transactions on Smart Grid*, 3(4):1832–1840, Dec 2012.

[13] L. Shalalfeh, P. Bogdan, and E. Jonckheere. Evidence of long-range dependence in power grid. In *2016 IEEE Power and Energy Society General Meeting (PESGM)*, pages 1–5, July 2016.

[14] H. Lavicka and J. Kracik. Fluctuation analysis of electric power loads in Europe: correlation multifractality vs. distribution function multifractality. arXiv:1706.00467v1 [q-fin.ST], June 2017.

[15] M. Pignati, M. Popovic, S. Barreto, R. Cherkaoui, G. Dario Flores, J. Y. Le Boudec, M. Mohiuddin, M. Paolone, P. Romano, S. Sarri, T. Tesfay, D. C. Tomozei, and L. Zanni. Real-time state estimation of the epfl-campus medium-voltage grid by using pmus. In *2015 IEEE Power Energy Society Innovative Smart Grid Technologies Conference (ISGT)*, pages 1–5, Feb 2015.

[16] PMU data from EPFL campus. http://nanotera-stg2.epfl.ch/. [Online; accessed 14-May-2018].

[17] C.-K. Peng et al. Mosaic organization of DNA nucleotides. *Phys Rev E*, 49(2), 1994.

[18] A. Eke, P. Herman, J. B. Bassingthwaighte, G. Raymond, D. Percival, M. J. Cannon, I. Balla, and C. Ikenyi. Physiological time series: distinguishing fractal noises from motions. *Pflugers Archives - Eur J Physiol*, 439:403–415, 2000.

TABLE V. Values of the two information criteria (AIC and BIC) for multiple ARFIMA models of voltage time series from EPFL campus grid.

Model	AR parameters (Φ_1, Φ_2)	MA parameters (Θ_1, Θ_2)	Differencing parameter (d)	AIC	BIC
$(0, d, 0)$	$(0.00, 0.00)$	$(0.00, 0.00)$	1.23	-739.8	-725.0
$(1, d, 0)$	$(0.48, 0.00)$	$(0.00, 0.00)$	0.85	-832.2	-812.6
$\mathbf{(0, d, 1)}$	$\mathbf{(0.00, 0.00)}$	$\mathbf{(-0.63, 0.00)}$	$\mathbf{0.89}$	$\mathbf{-946.9}$	$\mathbf{-927.3}$
$(1, d, 1)$	$(0.03, 0.00)$	$(-0.62, 0.00)$	0.87	-945.1	-920.5
$(2, d, 0)$	$(0.41, -0.31)$	$(0.00, 0.00)$	1.07	-915.9	-891.3
$(0, d, 2)$	$(0.00, 0.00)$	$(-0.65, -0.02)$	0.87	-945.1	-920.6
$(2, d, 1)$	$(0.04, -0.06)$	$(-0.57, 0.00)$	0.91	-944.0	-914.6
$(1, d, 2)$	$(-0.88, 0.00)$	$(-1.54, -0.59)$	0.88	-946.0	-916.5
$(2, d, 2)$	$(-0.73, -0.07)$	$(-1.35, -0.50)$	0.90	-944.3	-909.9

TABLE VI. Values of the two information criteria (AIC and BIC) for multiple ARFIMA models of frequency time series from EPFL campus grid.

Model	AR parameters (Φ_1, Φ_2)	MA parameters (Θ_1, Θ_2)	Differencing parameter (d)	AIC	BIC
$(0, d, 0)$	$(0.00, 0.00)$	$(0.00, 0.00)$	0.47	-13512.0	-13497.3
$(1, d, 0)$	$(-0.36, 0.00)$	$(0.00, 0.00)$	0.62	-13607.7	-13588.1
$(0, d, 1)$	$(0.00, 0.00)$	$(0.61, 0.00)$	0.84	-13633.0	-13613.4
$(1, d, 1)$	$(-0.08, 0.00)$	$(0.62, 0.00)$	0.88	-13634.6	-13610.1
$(2, d, 0)$	$(-0.51, -0.18)$	$(0.00, 0.00)$	0.70	-13628.0	-13603.5
$(0, d, 2)$	$(0.00, 0.00)$	$(0.65, -0.05)$	0.83	-13634.1	-13609.6
$(2, d, 1)$	$(-0.04, 0.06)$	$(0.72, 0.00)$	0.94	-13633.7	-13604.3
$\mathbf{(1, d, 2)}$	$\mathbf{(-0.92, 0.00)}$	$\mathbf{(-0.18, 0.61)}$	$\mathbf{0.94}$	$\mathbf{-13645.5}$	$\mathbf{-13616.0}$
$(2, d, 2)$	$(-0.89, 0.02)$	$(-0.16, 0.60)$	0.93	-13643.7	-13609.4

TABLE VII. Values of the two information criteria (AIC and BIC) for multiple ARFIMA models of phase angle time series from EPFL campus grid.

Mode	AR parameters (Φ_1, Φ_2)	MA parameters (Θ_1, Θ_2)	Differencing parameter (d)	AIC	BIC
$(0, d, 0)$	$(0.00, 0.00)$	$(0.00, 0.00)$	0.17	-29399.1	-29384.3
$(1, d, 0)$	$(-0.18, 0.00)$	$(0.00, 0.00)$	0.83	-29418.7	-29399.1
$(0, d, 1)$	$(0.00, 0.00)$	$(0.18, 0.00)$	0.83	-29420.8	-29401.2
$\mathbf{(1, d, 1)}$	$\mathbf{(-0.18, 0.00)}$	$\mathbf{(0.18, 0.00)}$	$\mathbf{0.83}$	$\mathbf{-29543.0}$	$\mathbf{-29518.5}$
$(2, d, 0)$	$(-0.18, 0.02)$	$(0.00, 0.00)$	0.83	-29414.1	-29389.6
$(0, d, 2)$	$(0.00, 0.00)$	$(0.18, -0.02)$	0.83	-29418.5	-29394.0
$(2, d, 1)$	$(-0.18, 0.02)$	$(0.18, 0.00)$	0.83	-29537.4	-29507.9
$(1, d, 2)$	$(-0.18, 0.00)$	$(0.18, -0.02)$	0.83	-29538.6	-29509.1
$(2, d, 2)$	$(-0.18, 0.02)$	$(0.18, -0.02)$	0.83	-29532.5	-29498.2

[19] E. Stroe-Kunold, T. Stadnytska, J. Werner, and S. Braun. Estimating long-range dependence in time series: an evaluation of estimators implemented in R. *Behavior Research Methods*, 41:909–923, 2009.

[20] C. W. J. Granger and R. Joyeux. An introduction to long-range time series models and fractional differencing. *Journal of Time Series Analysis*, 1:15–30, 1980.

[21] G. E. P. Box and G. M. Jenkins. *Time Series Analysis: Forecasting and Control*. Holden-Day, Merrifield, Va., 1976.